Effects of Rhizosphere Microbial Composition on the Growth of *Cajanus Cajan* in Coal Gangue Reclaimed Soil

Shiming Han
Liupanshui Normal University
Yuexia Wang
Liupanshui Normal University
Rongcan Zou
Liupanshui Enviromental engineering assessment center
Boqiu Wang
Liupanshui Normal University
kaiyi shi (andrewshikai@126.com)
Hechi University https://orcid.org/0000-0001-9705-9022

Methodology

Keywords: ecological management, Microorganisms, ecological restoration, bacterial and fungal biodiversity, Robillarda

Posted Date: August 2nd, 2021

DOI: https://doi.org/10.21203/rs.3.rs-738795/v1

Abstract

Planting the economically sustainable *Cajanus cajan* crop in coal gangue dump as an approach for ecological management has attracted extensive attention from scholars worldwide. Microorganisms play important roles in ecological restoration. However, there have been few reports about the microbial composition and functions of *Cajanus cajan* root systems planted in plateau waste dumps. In this study, the gangue dump (1,390 m above sea level) in Guizhou Plateau was covered with soil and planted with YN and JX *Cajanus cajan*s. After one year, the *Cajanus cajan* root system was collected, and high-throughput sequencing was utilized to examine the bacterial and fungal biodiversity. The bacteria in all samples were assigned to six phyla and 60 genera. The *unclassified_f_Enterobacteriaceae* and *Cedecea* were the most abundant genera. The fungi were assigned to six phyla and 143 genera and *Fusarium* was the most abundant genus. Venn and heatmap analyses revealed differences in the dominant root species among *Cajanus cajan* varieties, *Lactococcus* and *Fusarium.* In JX and YN, *Pseudoarthrobacter* is a unique genus of bacteria; in JX, *Robillarda* is a unique genus of fungi; and in YN, *Scytalidium* is a unique genus of fungi. The *endophytic* fungi mainly play the roles of saprotroph, plant pathogen, and endophyte. Among the bacterial properties, L-arabinose isomerase and adenosine triphosphatase were the most abundant in all samples, while chitinase, catalase, and laccase played important roles in photosynthesis, degradation of lignin, chitin, and chitosan. This study guides the selection of reclamation plants and strategies for the migration and restriction of heavy metals in soil.

Introduction

Coal gangue is extracted from rock interlayers during coal mining and is discharged during coal washing and processing (**Wu *et al.*, 2021**). However, its use is restricted due to the low carbon content and high cost of resource utilization, and most coal mining enterprises must pile up in the vicinity of the mining area for a long time, which occupies a lot of land and seriously impacts the surrounding ecological environment, which causes social and environmental problems (**Zhou *et al.*, 2021**). In recent years, due to the development of the economy and the emphasis on the ecological environment, ecological restoration of gangue hills has attracted the attention of researchers and has become a hotspot for studies on the ecological restoration of mining areas(**Lang *et al.*, 2002; Wang *et al.*, 2019; Zhang *et al.*, 2020**).

Natural remediation of gangue mountain is a remarkably slow process that takes between 50 to 100 years to achieve natural restoration, since gangue mountain soil belongs to inferior soil, which is not conducive to plant growth. Therefore, many countries began using artificial intervention for the ecological restoration of waste hills. In the United States, Germany, Australia, and other coal mining regions, the ecological restoration of coal gangue was carried out in earlier time periods. In the 1920s, Germany began growing plants on gangue hills and gradually established the landscape ecology of mining areas (**Lang *et al.*, 2002**). In the 1970s, the United States established the mining guarantee system, which issued a financial guarantee for the ecological restoration of mining areas (**Asif & Chen, 2015; Song, 2011**). Australia has made remarkable achievements in landscape restoration, waste management, and biodiversity conservation (**Waggitt *et al.*, 2006**). In the early 1980s, China began managing the ecological environment of mines, which involved studying the treatment of three types of wastes and land reclamation (**Zhao *et al.*, 1990**).

Land reclamation is one of the most effective methods for ecological restoration of mining areas (**Bulgarelli *et al.*, 2015**; **Wang & Li, 2013**). The reclamation rate of mining areas in the United States is over 85%, and vegetation and land after land reclamation have been restored to their original states. Thus, land reclamation plays an important role in restoring the ecology of mining areas and reducing the impacts of mining pollution on the environment. For the development and implementation of land reclamation of mining areas, scholars around the world have studied land shaping, plant species screening, and soil physical and chemical properties. Throughout the long-term research and field planting practice, several principles of plant variety selection, such as the ecological adaptability principles, pioneering principles, resistance principles, and biodiversity principles, have been described.

According to the above principles, planting dal, or '*Cajanus cajan*,' on coal gangue hills has been an effective ecological restoration method. The soil of gangue hills is loose and prone to landslide. Therefore, the short above-ground part and developed root system of the dal plant allows *Cajanus cajan* to grow rapidly and cover the slope surface within a short time period, which is beneficial for soil fixation and greening of gangue hills. However, because gangue hill soil contains certain combustible coal, the soil temperature rises to high temperatures under the sunshine condition, which is not conducive to plant growth. Furthermore, coal gangue has a low water retention rate, which is not conducive to direct plant growth. Water shortage and dryness can be solved by planting plants after overlaying the gangue hills with soil. On the one hand, it can greatly improve the soil composition of gangue hills and provide basic components to enhance plant growth. On the other hand, plant roots pass through the overlying soil and enter the gangue layer, which plays a role in soil consolidation of the gangue layer. **Tan (2016)** evaluated the soil heavy metal pollution remediation of *Robinia pseudoacacia*, white elm, *Pinus camphoris*, Torchbladellia, etc. in Fushun Gangue Hill. **Brown *et al* (1995)** grew *Silene vulgaris* in a mine contaminated with heavy metals and found that it was damaged only when the Zn content was higher than 0.32 mM. **Muller *et al* (2000)** studied three kinds of heavy metal detoxification and tolerance of *Armeria maritima* ssp. *halleri*, *Cardaminopsis halleri,* and *C. alleri* . **Yao *et al* (2021)**. analyzed the planting prospect of *Cajanus cajan* in rocky desertification soil.

Most scholars have focused on the selection of plants used in the reclaimed soil of gangue hills and the enrichment of heavy metals by plants. However, there have been few reports on the microbial diversity of plant roots. Therefore, in this paper, the reclaimed plant *Cajanus cajan* of Coal Gangues Hill in Liupanshui was the research object. The root microorganisms were systematically analyzed by high-throughput sequencing technology, and the functions of related microorganisms were preliminarily analyzed to provide a theoretical basis for the interaction mechanism between reclaimed plants and gangue hills.

Materials And Methods

Coal Gangue and Planting

The gangue storage yard of Panzhou Juneng Coal Preparation Co., Ltd. is located in Panzhou, Guizhou, China. It is 25°25'54 "N, 104°36'7" E, 1,390 m above sea level, with an annual average temperature of 16°C and an annual rainfall of 1,400 mm. On March 27, 2019, the project team sorted the gangue mountain into a gentle slope terrain with an inclination of less than 45° and covered the surface of the gangue with red soil at

a depth of 15 cm ~ 30 cm. On April 3, 2019, JX and YN *Cajanus cajan* seeds were planted in 1 m intervals of *Cajanus cajan* from different habitats and were watered one to two times per week.

Measurement of *Cajanus cajan* growth

After JX and YN *Cajanus cajan* seeds were planted, the saplings were measured by tape measure. Ten plants of each variety were tested and the average value was taken. Then, the growth curve of different varieties of *Cajanus cajan* saplings were drawn.

Collection and Treatment of Soil Samples

On July 25, 2020, the roots of soil-covered *Cajanus cajan* JX and YN were collected as follows: The soil was dug with a disinfected shovel. Most roots were deep into the soil by more than 70 cm, and large pieces of soil were stripped off the roots. The samples were packed in sample bags and brought to the laboratory where they were stored at a low temperature until further treatment. The roots of the *Cajanus cajan* were washed with sterile water, rinsed until the topsoil was clean, and then sterile hand scissors were used to cut the samples into pieces. The samples were then stored in a refrigerator maintained at -80°C.

DNA extraction and PCR amplification

Microbial community genomic DNA was extracted from *Cajanus cajan* Root samples using the E.Z.N.A.® soil DNA Kit (Omega Bio-tek, Norcross, GA, U.S.) according to manufacturer's instructions. The DNA extract was checked on 1% agarose gel, and DNA concentration and purity were determined with NanoDrop 2000 UV-vis spectrophotometer (Thermo Scientific, Wilmington, USA). As for the bacterial flora, the hypervariable region V5-V7 of 16S rRNA gene were amplified by an ABI GeneAmp® 9700 PCR thermocycler (ABI, CA, USA) in two rounds. in the first round, primers 799f (799F(5´-AACMGGA TTAGA TACCCKG-3´) and 1392R (5-ACGGGCGGTGTRC-3) were used, and the number of cycles was 27. In the second round, 799F (5'-AACMGGA TTAGA TACCCKG-3') and 1193r (5'-ACG TCA TCC CCCCT TCC-3') were used with a cycle number of 13 (**Bulgarelli *et al.*, 2012; Bulgarelli *et al.*, 2015**). The PCR amplification of 16S rRNA gene was performed as follows: initial denaturation at 95 ℃ for 3 min, annealing at 55 ℃ for 30 s and extension at 72 ℃ for 30 s, and single extension at 72 ℃ for 10 min, and end at 4 ℃. As for Endophytic Fungi, ITS1 region was amplified with primer pairs ITS1F (5'-CTTGGTCATTTAGAGGAAGTAA-3') and ITS2R (5'-GCTGCGTTCTTCATCGATGC-3') by an ABI GeneAmp® 9700 PCR thermocycler (ABI, CA, USA) (**Adams *et al.*, 2013**). The PCR amplification was performed as follows: initial denaturation at 95 ℃ for 3 min, followed by 27 cycles of denaturing at 95 ℃ for 30 s, annealing at 55 ℃ for 30 s and extension at 72 ℃ for 30 s, and single extension at 72 ℃ for 10 min, and end at 4 ℃ (**Davide *et al.*, 2012**).

The PCR mixtures contain 5 × TransStart FastPfu buffer 4 μL, 2.5 mM dNTPs 2 μL , forward primer (5 μM) 0.8 μL, reverse primer (5 μM) 0.8 μL, TransStart FastPfu DNA Polymerase 0.4 μL, template DNA 10 ng, and finally ddH2O up to 20 μL. PCR reactions were performed in triplicate. The PCR product was extracted from 2% agarose gel and purified using the AxyPrep DNA Gel Extraction Kit (Axygen Biosciences, Union City, CA, USA) according to manufacturer's instructions and quantified using Quantus™ Fluorometer (Promega, USA).

Illumina MiSeq sequencing

Purified amplicons were pooled in equimolar and paired-end sequenced on an Illumina MiSeq PE300 platform/NovaSeq PE250 platform (Illumina, San Diego,USA) according to the standard protocols by Majorbio Bio-Pharm Technology Co. Ltd. (Shanghai, China). The raw reads were deposited into the NCBI Sequence Read Archive (SRA) database (Accession Number: SRR14778041、SRR14777823、SRR14777774、SRR14777775、SRR14777776、SRR14777777、SRR14777778、SRR14777779、SRR14777551、SRR14777552、SRR14777553).

Processing of sequencing data

The raw 16S rRNA gene sequencing reads were demultiplexed, quality-filtered by fastp version 0.20.0 and merged by FLASH version 1.2.7 with the following criteria (**Chen *et al.*, 2018; Magoč *et al.*, 2011**): (i) the 300 bp reads were truncated at any site receiving an average quality score of <20 over a 50 bp sliding window, and the truncated reads shorter than 50 bp were discarded, reads containing ambiguous characters were also discarded; (ii) only overlapping sequences longer than 10 bp were assembled according to their overlapped sequence. The maximum mismatch ratio of overlap region is 0.2. Reads that could not be assembled were discarded; (iii) Samples were distinguished according to the barcode and primers, and the sequence direction was adjusted, exact barcode matching, 2 nucleotide mismatch in primer matching.

Operational taxonomic units (OTUs) with 97% similarity cutoff were clustered using UPARSE version 7.1 (**Edgar, 2013; Stackebrandt & Goebel, 1994**), and chimeric sequences were identified and removed. The taxonomy of each OTU representative sequence was analyzed by RDP Classifier version 2.2 against the 16S rRNA database (eg. Silva v138) and ITS1 rRNA database (unite8.0/its_fungi) using confidence threshold of 0.7 (**Wang *et al.*, 2007**).

Results And Analysis

Growth curve of *Cajanus cajan*

The growth curve of YN and JX *Cajanus cajan* saplings were shown in **Figure 1**. The saplings growth height of each variety was relatively uniform, and the standard error was between 0.03 and 1.11 cm. YN *Cajanus cajan* shows better growth rate than JX *Cajanus cajan, i*n the 8th month, the average height of YN seedlings was 314.97 cm, while that of JN was only 295.34 cm.

Sequence Length Distribution

16S rDNA sequencing of bacteria in six samples showed that 145,496 base pairs were detected, with the lowest length of 219 bp, the longest length of 407 bp, and an average length of 377 bp. A total of 96,563,333 base pairs were detected in the ITS1F_ITS2R region of 18S rDNA, which ranged from 140 bp to 300 bp in length, with an average length of 225 bp.

Operational Taxonomic Unit Species Classification Statistics

Analysis of root soil samples showed that bacteria had one domain, 1 kingdom, 6 phyla, 8 classes, 23 orders, 41 families, 60 genera, 67 species, and 72 operational taxonomic units (OTUs), while fungi had one domain,

1 kingdom, 6 phyla, 21 classes, 49 orders, 94 families, 143 genera, 180 species, and 266 OTUs.

Analysis of the Alpha Diversity of Samples

As can be seen from the dilution curve of the fungal samples (**Figure 2A**), when the sample sequence increased to more than 30,000, the Shannon index curve was almost flat, which indicated that the sequencing volume continued to increase. The number of newly added OTUs exhibited a limited increase. The number of experimental sequences in the experiment reached 70,000, which was a sufficient amount of data for the analysis. The dilution curve of the bacterial samples (**Figure 2B**) indicated that the sequencing amount was about 3,000, the OTUs of all the experiments increased gradually, and the sequencing amount was sufficient. **Figure 2C and 2D** depicts the uniformity curve of the sample. It can be seen that the Heip curve of fungi was very steep. When the sample number reached 21,000, the Heip index reduced to 0.02, which indicated that the homogeneity of the fungi is remarkably high. **Figure 2D** shows that the Heip curve was steep, which indicated high uniformity of the sample.

After coal gangue covered the soil, JX *Cajanus cajan* and YN *Cajanus cajan* were planted with an ace index and Chao index of 0.5354 and 0.6568, respectively, which were each greater than 0.05, thus indicating that no significant difference in their microbial diversity,. The *P* values of the ace index and Chao index of fungi were 0.00899 and 0.00793, respectively, which were each less than 0.01, thus indicating significant differences in the root fungi of the different varieties of chime bean that were planted, as shown in **Table 1** and **Figure 3**).

Table 1. microbial diversity of JX pigeon pea and YN Pigeon pea

Group	index	JX-Mean	JX-Sd	YN-Mean	YN-Sd	P
fungi	ace	93.762	7.5163	121.79	6.932	0.00899
	chao	92.609	8.5551	120.14	4.5529	0.00793
bacteria	ace	51.57	15.35	44.807	7.9777	0.5354
	chao	44.688	12.545	40.676	7.2664	0.6568

Species Composition Analysis

Figure 4 compares the differences between the bacteria and fungi in the microbial composition of different varieties of *Cajanus cajan* roots at the genus level of the samples. According to a Venn diagram, there were 38 genera of bacteria in two different varieties of *Cajanus cajan*, among which *unclassified_f_Enterobacteriaceae* and *Cedecea* were the dominant genera, accounting for 31.0% and 29.8%, respectively. The unique bacteria of JX and YN *Cajanus cajan* belong contained 15 genera and 10 genera, respectively, and the dominant genera are *Lactococcus* and *Pseudomonas* bacteria, which account for 25.0% and 29.5%, respectively. The Venn diagram of the fungi showed that there were 84 genera of fungi in the root soil of two kinds of *Cajanus cajan*, among which *Fusarium* was the dominant strain, accounting for 41.2%, followed by *Acrocalymma* and *Neocosmospora*, which accounted for 19.9% and 14.8%, respectively. Twenty-two genera of fungi are unique to JX *Cajanus cajan*, among which *Robillarda* is the dominant strain,

accounting for 91.8%. There were 37 genera of fungi in YN *Cajanus cajan*, and the dominant fungus was *Scytalidium*, accounting for 41.2%, which can cause infection. The second- and third-most dominant fungi were *Herpotrichiellaceae* and *Acidomyces*, accounting for 17.9% and 14.8%, respectively (**Mendoza *et al.*, 2009**).

Heat Map Analysis of Bacterial Colony Composition at the Genus Level

Species with the top 20 total abundance at the genus level of classification were selected to display variation in the abundance of different species in samples through a color gradient of color blocks. **Figure 5** depicts a heat map of bacteria at the genus level. It can be seen from the figure that *Enterobacteriaceae* and *Cedecea* were dominant bacteria genera in the six samples, and the abundances of Yng1 and Yng2 were also remarkably high. **Figure 5** depicts the heat map of fungi at the level of genus classification. It can be seen from the figure that, except *Fusarium*, the distribution of other fungi in each sample was very significant. *Acrocalymma* in JX *Cajanus cajan* (samples Jxg1, Jxg2, and Jxg3) was also one of the dominant genera. The root microorganisms of different *Cajanus cajan* varieties have significant differences.

Phylogenetic Tree Analysis of rhizobacteria

Phylogenetic trees were constructed at the genus level to explore the phylogenetic correlation of the dominant strains, as shown in **Figure 6**. On the left is the phylogenetic evolutionary tree, in which each branch represents a class of species, and the branches are colored according to the advanced taxonomic level to which the species belongs. The length of the branch was the evolutionary distance between two species. The bar chart on the right shows the proportion of reads for different groups of species. As can be seen from the phylogenetic tree of bacteria, the homology of the dominant strains *Enterobacteriaceae*, *Cedecea*, *Enterobacter*, *Pantoea*, and *Candidatus Phytoplasma* is poor, with significant differences among the species.

According to the phylogenetic tree of fungi (**Figure 7**), the dominant strains *Acrocalymma* and *Setophoma* had high homology; *Neocosmospora* and unclassified *Nectriaceae* had high homology, and *Fusarium* had low homology, with significant differences in comparison with other dominant strains.

Functional Analysis of Microorganism

Based on the published literature or data from authoritative websites, fungal communities in the samples were classified and analyzed using microecology Guild, and functional classification of fungi was performed using FUNGuild software to obtain information on the functional classification of fungi in samples and the abundance of each functional classification in the different samples, as shown in **Figure 8**. According to the figure, the main functions of endophytes at the root of *Cajanus cajan* were saprotroph, plant Pathogen, and endophyte.

The COG family information and KEGG Orthology (KO) information corresponding to the OTU were obtained according to the greengene ID corresponding to each OTU in the samples, and the abundance of each COG and KO were calculated. The amplicon sequencing data for the fungal ITS can be used for functional prediction. The result is shown in **Figure 9**. It can be seen from the figure that L-arabinose isomerase (5.6.1.4)

and adenosine triphosphatase (3.1.6.3) have the highest abundance among the six samples, followed by chitosanase (3.2.1.132), chitinase (3.2.1.14), catalase (1.11.1.6), peroxidase (1.11.1.7), monooxygenase (1.14.14.1), laccase (1.10.3.2), nitrilase (3.5.5.1), Acid phosphatase (3.1.3.2) (**Hui, 2019; Jin *et al.*, 2020; Sun, 2019**).

How to maintain the plant's long-term survival so that it becomes the dominant plant is a key to ecological restoration of coal gangue. Therefore, plant growth is related to soil nutrient sources and is related to endophytic microorganisms. Endophytic bacteria can produce a variety of active substances through metabolism, which can promote the growth and development of host plants and improve the resistance of host plants. Endophytic microorganisms may be pathogenic microorganisms that can harm plant growth. Therefore, it is critical to study the endophytic bacteria of caesium in the reclamation plant on gangue mountain.

Discussion

Differences in the Endophytic Bacteria of Different Varieties of Cajanus cajan

Based on the Venn diagrams, *unclassified_f_Enterobacteriaceae* and *Cedecea* were dominant bacteria, among which *Enterobacteriaceae* formed a large group of gram-negative bacteria living in human and animal intestines, most of which belonged to normal flora, although there were some pathogenic bacteria that can cause human and animal infections. Markova isolated *Enterobacteriaceae* from wild pear (*Pyrus pasha*) and other plant tissues (Markova et al., 2005). *Cedecea* is an *Enterobacterium* that degrades organic matter, as was reported by **Cao** et al **(2019**). The unique dominant bacteria of JX *Cajanus cajan* is *Lactococcus*, which produces organic acid, hydrogen peroxide, bacteriocin, and other substances that inhibit the growth of spoilage bacteria during the metabolism of fermented sugar. Among the unique dominant fine bacteria evaluated by Wang, *Lactococcus* was isolated from *Kefir* grain. The unique dominant bacteria YN *Cajanus cajan* is *Pseudarthrobacter*, which is abundant in contaminated soil and can degrade contaminated organic matter in soil (Wang et al., 2015). Fekih et al (2018)Ben reported the features and draft genome sequence of *Pseudarthrobacter sp*. strain AG30, which was isolated from the Zijin gold and copper mine in China. The richness of endophytic fungi in *Cajanus cajan* was higher than that of bacteria, with only 72 OTUs in bacteria and 266 OTUs in fungi. According to the Venn diagram of fungi, *Fusarium* was the dominant symbiotic fungi, accounting for 41.2%, followed by *Acrocalymma* and *Neocosmospora*, which accounted for 19.9% and 14.8%, respectively. *Fusarium* is an important pathogen that causes seedling disease, root rot, and pre- and post-emergence damping-off (Chiotta et al., 2021). Cruz analyzed the effects of soil conditions (soil texture, pH, and soil moisture) on *Fusarium graminearum* when planting (Jimenez et al., 2020). Parroni et al (2019) reported the use of *Trametes versicolor* for Controlling the cereal pathogen *Fusarium langsethiae*. Wei (2019**)** screened for *Acrocalymma* from soil around the coal mine and found that *Acrocalymma* formed a symbiotic relationship with alfalfa and sand Holly and promoted the uptake of nitrogen and phosphorus by plants. Jin et al (2017) found that *Acrocalymma* reduced the heavy metal content in tobacco leaves. *Neocosmospora* is a fungus that can remove heavy metals. Giovanni et al (2020) reported that the *Neocosmospora* sp. strain secreted specific novel phenolic compounds in response to lead exposure. Yang et al (2017) reported *Setophoma* could cause pink root rot on canola

Effects of rhizosphere microbial composition on the growth of Cajanus cajan

The height of *Cajanus cajan* saplings was correlated with the root microorganism, and the heat map was drawn as shown in Fig. 10. It can be seen from Fig. 10 that the microbial composition of high strain *Cajanus cajan* (YN) and low strain *Cajanus cajan* (JX) is significantly different. *Setophoma, neocosmospora, Rhizoctonia*, and *Fusarium* were positively correlated. While *acrocalymma, nectriaceae, clonostachys* were negatively correlated.

Functional Analysis of Endophytic Fungi

Using the software FUNGuild to analyze the microecology of fungi, it was determined that different samples have three main functions: saprotroph, plant pathogen, and endophyte. The microecological functions of different varieties of fungi were different, among which, the undefined saprotrophic bacteria content in YN *Cajanus cajan* was highest (47.94%), whereas in YN *Cajanus cajan*, it was lowest (41.14%). Endophyte fungi were equally abundant in two kinds of lignans at 40.57% and 40.47%, respectively. The proportion of plant pathogenic bacteria in YN *Cajanus cajan* was twice that of JX, at 8.18% and 4.00%, respectively. In addition, wood saprotrophic fungi accounted for 4.90% in JX *Cajanus cajan* and 0% in YN *Cajanus cajan*. Plant pathogenic fungi are harmful and cause *Cajanus cajan* infection, which enables the *Cajanus cajan* to grow better in dirt and gangue mounds (Nick et al., 2020). Saprotrophic bacteria can be both beneficial and harmful. Wood saprotrophs can decompose dead branches and leaves, which further breaks down the plant and is thus known as a growth nutrient for *Cajanus cajan*. On the other hand, the bacteria can also rot the *Cajanus cajan* root, thereby negatively affecting its growth. Endophyte has many benefits for plant growth, including nitrogen fixation (Lyons et al., 1990), growth promotion(Shahzad et al., 2016;Singh et al., 2013), and resistance to pests (Hossain et al., 2016) and nonliving organisms (Santos et al., 2017; Zhou et al., 2020). At present, studies on the extraction of bioactive substances such as alkaloids, peptides from endophytes (**Gary** et al., **2014; Yu** et al., **2021)**, biological fertilizers (Pham et al., 2017), biological pesticide preparations, and so on, have become a research hotspot. Therefore, it is important to study the influence of endophytic bacteria on the vegetation of waste rocks that are rich in heavy metals. In the next step, we will further study the migration and adsorption of heavy metals from endophytes and gangue piles.

Functional Analysis of Endophytic Bacteria

The abundances of L-arabinose isomerase (5.6.1.4) and adenosine triphosphatase (3.1.6.3) were highest in fungi. Among them, the bioconversion of d-galactose was the effective enzyme of D-targose (Cheng et al., 2010), and adenosine triphosphatase was an essential enzyme involved in energy conversion and nutrient synthesis in photosynthesis and respiration, and thus plays a critical role in plants. Chitinase (3.2.1.14) hydrolyzes chitin (Hui, 2019**)**, while Chitosanase (3.2.1.132) hydrolyzes completely deacetylated chitosans(Jin et al., 2020). Catalase (1.11.1.6) and Peroxidase (1.11.1.7) are the most important enzymes involved in oxidation-reduction reactions, and they have catalytic effects on the decomposition of plant litter and the synthesis of humus (Sun, 2019**)**. Laccase (1.10.3.2) is an important enzyme that degrades lignin. Urease is an amide enzyme that plays a decisive role in the conversion of urea in soil. The activity of urease can represent the content of N in soil.

Abbreviations

KO KEGG Orthology

OTU Operational taxonomic units

Declarations

Ethics approval and consent to participate

We have stated that Ethics approval and consent to participate:No applicable.

Consent for publication

No applicable.

Competing interests

The authors declare that they have no competing interests.

Funding

This research was financially supported in part by the Research Foundation for Advanced Talents of Liupanshui Normal University (LPSSYKYJJ201601), the Liupanshui Key Laboratory for Research and Utilization of Characteristic Fruit Tree Resources (52020-2017-02-03), and
the Science and Technology Innovation Team Project of Liupanshui Normal University (LPSSYKJTD201602).

Authors' contributions

Shiming Han and Boqiu Wang performed the experiment, Yuexia Wang and Kaiyi Shi contributed significantly to analysis and manuscript preparation, Rongcan Zou helped perform the analysis with constructive discussions.

Acknowledgements

We appreciated Mr. Liu for his help in the sample test.

Availability of data and material

The raw reads were deposited into the NCBI Sequence Read Archive (SRA) database (Accession Number: SRR14778041、SRR14777823、SRR14777774、SRR14777775、SRR14777776、SRR14777777、SRR14777778、SRR14777779、SRR14777551、SRR14777552、SRR14777553).

References

1. Adams, R. I., Miletto, M., Taylor, J. W., & Bruns, T. D. (**2013**) Dispersal in microbes: fungi in indoor air are dominated by outdoor air and show dispersal limitation at short distances. *The ISME Journal.* 7(7),1262-

1273. https://doi.org/10.1038/ismej.2013.28

2. Asif, Z. , & Chen, Z. (**2015**). Environmental management in north american mining sector. *Environmental Science & Pollution Research International*, 23(1), 167-179. https://doi.org/10.1007/s11356-015-5651-8
3. Brown, S. L. , Chaney, R. L. , Angle, J. S. , Baker, A. J. M. (**1995**). Zinc and cadmium uptake by hyperaccumulator thlaspi caerulescens and metal tolerant silene vulgaris grown on sludge-amended soils. *Environmental Science & Technology*, 29(6), 1581-5. https://doi.org/10.1021/es00006a022
4. Bulgarelli, D., Rott, M., Schlaeppi, K. et al. (**2012**) Revealing structure and assembly cues for Arabidopsis root-inhabiting bacterial microbiota. *Nature*, 488, 91–95. https://doi.org/10.1038/nature11336
5. Bulgarelli D, Garrido-Oter R, Münch P C, et al. (**2015**). Structure and function of the bacterial root microbiota in wild and domesticated barley. *Cell host & microbe*, 17(3), 392-403. https://doi.org/10.1016/j.chom.2015.01.011
6. Cao, D. J. , Wang, J. J. , Zhang, Q. , Wen, Y. Z. , Dong, B. , & Liu, R. J. , Yang X. Geng G. (**2018**). Biodegradation of triphenylmethane dye crystal violet by cedecea davisae. *Spectrochimica Acta Part A Molecular & Biomolecular Spectroscopy*, 210(5), 9-13. https://doi.org/10.1016/j.saa.2018.11.004
7. Chen, S., Zhou, Y., Chen, Y., & Jia, G. (**2018**). Fastp: an ultra-fast all-in-one fastq preprocessor. *Bioinformatics*, 34(17), i884-i890. https://doi.org/10.1093/bioinformatics/bty560
8. Cheng, L. , Mu, W. , Tao, Z. , & Bo, J.(**2010**). An l-arabinose isomerase from acidothermus cellulolytics atcc 43068: cloning, expression, purification, and characterization. *Applied Microbiology and Biotechnology*, 86(4), 1089-1097. https://doi.org/10.1007/s00253-009-2322-z
9. Chiotta, M. L. , Zanon, M. A. , Palazzini, J. M. , Alberione, E. , Barros, G. G. , & Chulze, S. N. . (**2021**). Fusarium graminearum species complex occurrence on soybean and f. graminearum sensu stricto inoculum maintenance on residues in soybean-wheat rotation under field conditions. *Journal of Applied Microbiology,* 130(1), 208-216(9). https://doi.org/10.1111/jam.14765
10. Muller D. H. , Oort, F. V. , Gélie B., Balabane, M. (**2000**). Strategies of heavy metal uptake by three plant species growing near a metal smelter. *Environmental Pollution*, 109(2), 231-238. https://doi.org/10.1016/S0269-7491(99)00262-6
11. Magoč T., Salzberg S. L. (**2011**) FLASH: fast length adjustment of short reads to improve genome assemblies. *Bioinformatics*, 27(21):2957-2963. doi:10.1093/bioinformatics/btr507
12. Davide, B., Matthias,R., Klaus, S., Emiel,V. L. T., Nahal, A., Federica, A., Philipp, R., Bruno, H., Richard, R., Elmon, S., Joerg, P., Frank, O. G., Rudolf, A., Thilo, E.& Paul, S. (**2012**). Revealing structure and assembly cues for arabidopsis root-inhabiting bacterial microbiota. *Nature,* 488, 91–95 https://doi.org/10.1038/nature11336
13. Edgar, R. C. (**2013**). Uparse: highly accurate otu sequences from microbial amplicon reads. *Nature Methods*, 10(10), 996. https://doi.org/10.1038/NMETH.2604
14. Fekih, I. B. , Ma, Y. , Herzberg, M. , Zhang, C. , Li, Y. P. , Mazhar, S. H., Bello S. K., Yang N., Su J., Xu J., Zhang R., Feng R., Chen Z., Rensing C.(**2018**). Draft genome sequence of pseudarthrobacter sp. strain ag30, isolated from a gold and copper mine in china. *Microbiology Resource Announcements*, 7(17), e01329-18. https://doi.org/10.1128/MRA.01329-18

15. Gary S., Bryn D., Uvidelio C., & James H. (**2004**). Natural products from endophytic microorganisms. *Journal of Natural Products*, 67(2), 257-268. https://doi.org/10.1021/np030397v
16. Hossain, M. T. , Khan, A. , Chung, E. J. , Rashid, H. O. , & Chung, Y. R. (**2016**). Biological control of rice bakanae by an endophytic bacillus oryzicola yc7007. *The Plant Pathology Journal*, 32(3), 228–241. https://doi.org/10.5423/PPJ.OA.10.2015.0218
17. Hui J.C. (**2019**). Highly active antibacterial mechanism of endophytic fungi of walnut filter and its metabolites (□). Dissertation: *Northwest A&F University*. (in Chinese)
18. Jimenez D. , Leandro, L. , Mayfield, D. A. , Y Meng, & Munkvold, G. P. (**2020**). Effects of soil conditions on root rot of soybean caused by fusarium graminearum. *Phytopathology*, 110(10), 1693-1703. https://doi.org/10.1094/PHYTO-02-20-0052-R
19. Jin H. Q. , Liu H. B. , Xie Y. Y. , Zhang Y. G., Xu Q. Q. , & Mao L. J., et al. (**2017**). Effect of the dark septate endophytic fungus acrocalymma vagum on heavy metal content in tobacco leaves. *Symbiosi*, 74, 89–95. https://doi.org/10.1007/s13199-017-0485-4
20. Jin Q. Z., Yan Z. L., Huang Z. Q., Yuan, H. Y., Liu, G. H, Nong, X. X., Li, X, & Luo, H. Y. (**2020**). Screening, identification and enzyme activity of endophytic fungi producing chitosanase. *Guangxi Botany*,40(9):1332-1340. (in Chinese)
21. Liang L. K., Chang J., Wu C.F., Klaus B. (**2002**). Sturdy on the ecological restoration of landscape in Germany mining regions and reference to China. *Economic Geography*, 22(6), 711-715. https://doi.org/10.15957/j.cnki.jjdl.2002.06.016
22. Lyons P. C. , Evans J. J. , & Bacon C. W. (**1990**). Effects of the fungal endophyte acremonium coenophialum on nitrogen accumulation and metabolism in tall fescue. *Plant Physiology*, 92(3), 726-32. https://doi.org/10.1104/pp.92.3.726
23. Markova Y. A., Romanenko A. S., & Dukhanina A. V. (**2005**). Isolation of bacteria of the family enterobacteriaceae from plant tissues. *Mikrobiologiia*, 74(5), 575-578. https://doi.org/10.1007/s11021-005-0105-9
24. Mendoza N. , Arora A. , Arias C. A. , Hernandez, C. A. , Madkam, V. , & Tyring, S. K. (**2009**). Cutaneous and subcutaneous mycoses. *Clinical Mycology (Second Edition)*, 509-523. https://doi.org/10.1016/B978-1-4160-5680-5.00024-4
25. Nick C., Snelders H. R., Gabriella C. P., Mercedes R., Grardy C. M. B., Julia A. V., Jeroen R. M., Michael F. S., Reindert N. & Bart P. H. J. T. (**2020**). Microbiome manipulation by a soil-borne fungal plant pathogen using effector proteins. *Nature Plants*, 6(11), 1-10. https://doi.org/10.1038/s41477-020-00799-5
26. Parroni A. , Bellabarba A. , Beccaccioli M. , Scarpari M. , Reverberi M. , & Infantino A. (**2019**). Use of the secreted proteome of trametes versicolor for controlling the cereal pathogen fusarium langsethiae. *International Journal of Molecular Sciences*, 20(17), 4167. https://doi.org/10.3390/ijms20174167
27. Pham V., Rediers H., Ghequire M., Nguyen H. H. , & Spaepen S. (**2017**). The plant growth-promoting effect of the nitrogen-fixing endophyte pseudomonas stutzeri a15. *Archives of Microbiology*, 199(3), 1-5. https://doi.org/10.1007/s00203-016-1332-3
28. Giovanni S., Flores-Vallejo R., Rivera-Leyva J., et al. (**2020**). Characterization of fungal endophytes isolated from the metal hyperaccumulator plant vachellia farnesiana growing in mine tailings.

Microorganisms, 8(2), 226. https://doi.org/10.3390/microorganisms8020226

29. Santos S., Silva P., Garcia A. C., JÉ Zilli & Berbara R. (**2017**). Dark septate endophyte decreases stress on rice plants. *Brazilian Journal of Microbiology*, 48(2), 333-341. https://doi.org/10.1016/j.bjm.2016.09.018
30. Shahzad R. , Waqas M. , Khan A. L. , Asaf S. , Khan M. A. , & Kang S. M. , et al. (**2016**). Seed-borne endophytic bacillus amyloliquefaciens rwl-1 produces gibberellins and regulates endogenous phytohormones of oryza sativa. *Plant Physiology & Biochemistry*, 236-243. https://doi.org/10.1016/j.plaphy.2016.05.006
31. Singh R. K. , Malik N. , & Singh S. (**2013**). Improved nutrient use efficiency increases plant growth of rice with the use of iaa-overproducing strains of endophytic burkholderia cepacia strain rre25. *Microbial Ecology*, 66, 375–384. https://doi.org/10.1007/s00248-013-0231-2
32. Sun Z. (**2019**). Effects of methyl methanesulfonate (MMS) and endophytic fungi treatment on rust resistance of Taibai poplar. Dissertation: *Northwest A&F University*. (in Chinese)
33. Song L. (**2011**). Establishment and reference of mine rehabilitation on deposit use in USA. *Resources & Industries*, 13(1), 166-172. https://doi.org/10.13776/j.cnki.resourcesindustries.2011.01.030
34. Stackebrandt E., Goebel B. M. (**1994**). Taxonomic Note: A Place for DNA-DNA Reassociation and 16S rRNA Sequence Analysis in the Present Species Definition in Bacteriology. *International Journal of Systematic Bacteriology*, 44(4):846-849. doi:10.1099/00207713-44-4-846
35. Tan W. S. (**2016**). Study on the remediation effect of different afforestation modes on soil heavy metal pollution in Fushun Gangue Hill. Dissertation: *Shenyang Agricultural University*. https://doi.org/10.1021/es00006a022 (in Chinese)
36. Waggitt P. (**2006**). Environmental regulation of uranium mining in Australia. In: Merkel B.J., Hasche-Berger A. (eds) Uranium in the Environment. Springer, *Berlin, Heidelberg*. https://doi.org/10.1007/3-540-28367-6_58
37. Wang C. X., Lu Y., Li Y. Y., Zhang B. C., Liang Y. B. (**2019**). Deformation process and prediction of filling gangue: A case study in China. *Geomechanics and Engineering*, 18(4), 417-426. https://doi.org/10.12989/gae.2019.18.4.417
38. Wang J. , Xing Z. , Tang W. , Zheng Y. , & Wang Y. (**2015**). Isolation, identification, and potential probiotic characterization of one lactococcus from kefir grain. *Food Science & Biotechnology*, 24(5), 1775-1780. https://doi.org/10.1007/s10068-015-0231-8
39. Wang Q. , Garrity G. M. , Tiedje J. M. , & Cole J. R. (**2007**). Naïve bayesian classifier for rapid assignment of rrna sequences into the new bacterial taxonomy. *Appl. Environ. Microbiol*, 73(16), 5261–5267. https://doi.org/10.1128/AEM.00062-07
40. Wang Y. , & Yan L. (**2013**). Land exploitation resulting in soil salinization in a desert–oasis ecotone. *Catena*, 100, 50–56. https://doi.org/10.1016/j.catena.2012.08.005
41. Wei J. (**2019**). Species diversity and heavy metal tolerance of DSE fungi in Fengfeng mining area, Hebei province. Dissertation: *Hebei University*. (in Chinese)
42. Wu J. X., Yan X. L, Li L., Gu J. H., Zhang T., Tian L. L., Su X. T., Lin Z. (**2021**). High-efficiency adsorption of Cr(VI) and RhB by hierarchical porous carbon prepared from coal gangue. *Chemosphere*, 275, http://dio.org/10.1016/J.CHEMOSPHERE.2021.130008

43. Yang, Y., Zuzak, K., Harding, M., Neilson, E., Feindel, D., & Feng, J. (**2017**). First report of pink root rot caused by Setophoma (Pyrenochaeta) terrestris on canola. *Canadian Journal of Plant Pathology*, 39(3), 354-360. doi:10.1080/07060661.2017.1355849
44. Yao Y., Zou R. C., Deng Q. T., He X. M., Gui L. L., Cao Z. X. (**2021**). Distribution Characteristics and Ecological Risk Assessment of Heavy Metals of Cajanus Cajan in Xiangshui Coal Gangue Repair Site, Liupanshui. *Environmental Impact Assessment*, 43(1), 80-85.
45. Yu Z., Zhao L. X. , Jiang C. L., Duan, Y., Wong L., & Carver K. C. , et al. (**2011**). Bafilomycins produced by an endophytic actinomycete streptomyces sp. yim56209. *Journal of Antibiotics*, 42(21), 159-162. https://doi.org/10.1002/chin.201121187
46. Zhang K., Xu L. J., Huang G. D., Meng X. Y., Yao J. X., Jiang B. X. (**2020**). Coupled variations of soil temperature and moisture in reclaimed fields filled with coal gangue of different grain size distributions. *Journal of Soils and Sediments*, 20(4), 2248-225. https://doi.org/10.1007/s11368-020-02579-2
47. Zhao J. C., Lv N. H., Li D. Z. (**1990**). Reclamation and planting of coal gangue. *Coal conversion*, (2), 1-5.
48. Zhou, J., Fu, Y. & Pan, S. (**2021**). The use of modified coal gangue for the remediation and removal of phosphorus in an enclosed water area. *Clean Technologies and Environmental Policy,* https://doi.org/10.1007/s10098-021-02026-x
49. Zhou J., Li P., Meng D., Gu Y., Zheng Z., Yin ., Zhou Q., Li J. (**2020**). Isolation, characterization and inoculation of cd tolerant rice endophytes and their impacts on rice under cd contaminated environment. *Environmental Pollution*, 260 (5), 113990. https://doi.org/10.1016/j.envpol.2020.113990

Figures

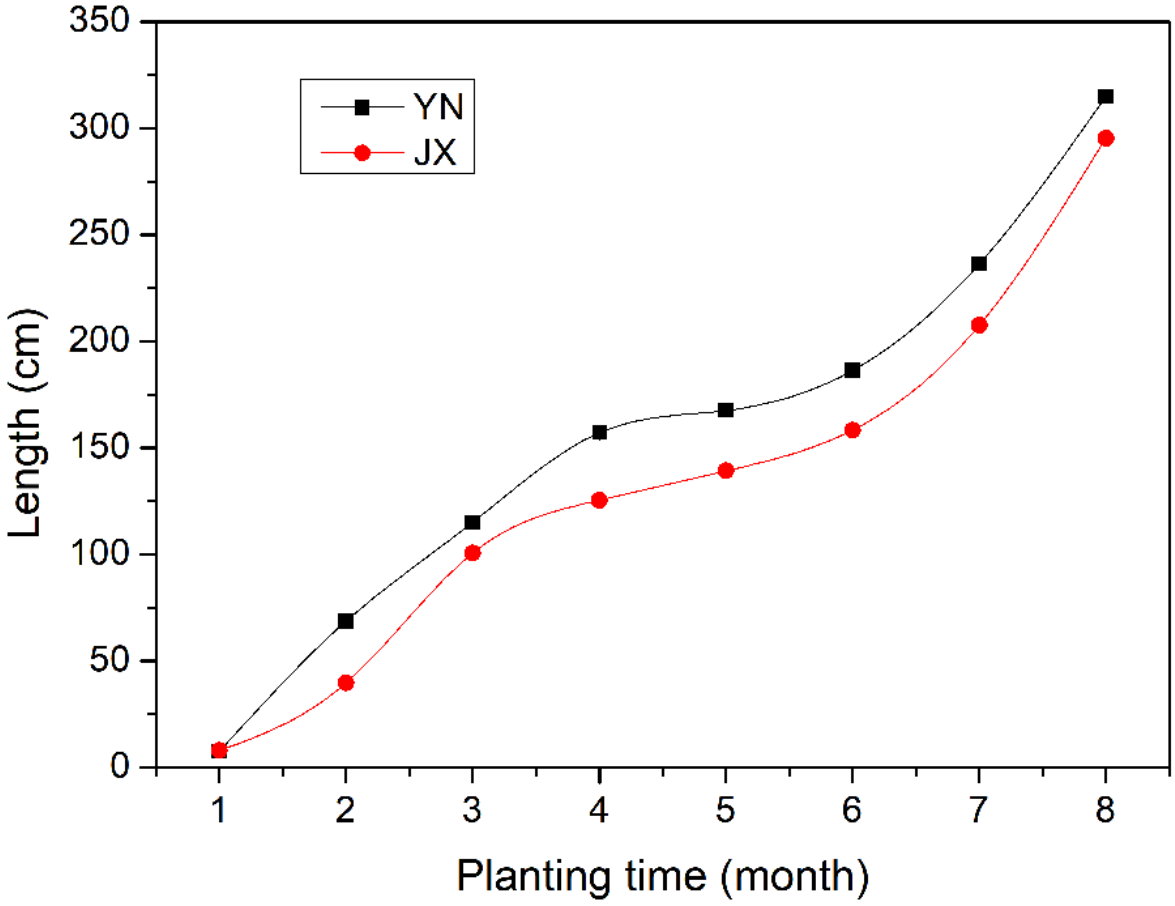

Figure 1

The growth curves of Cajanus cajan

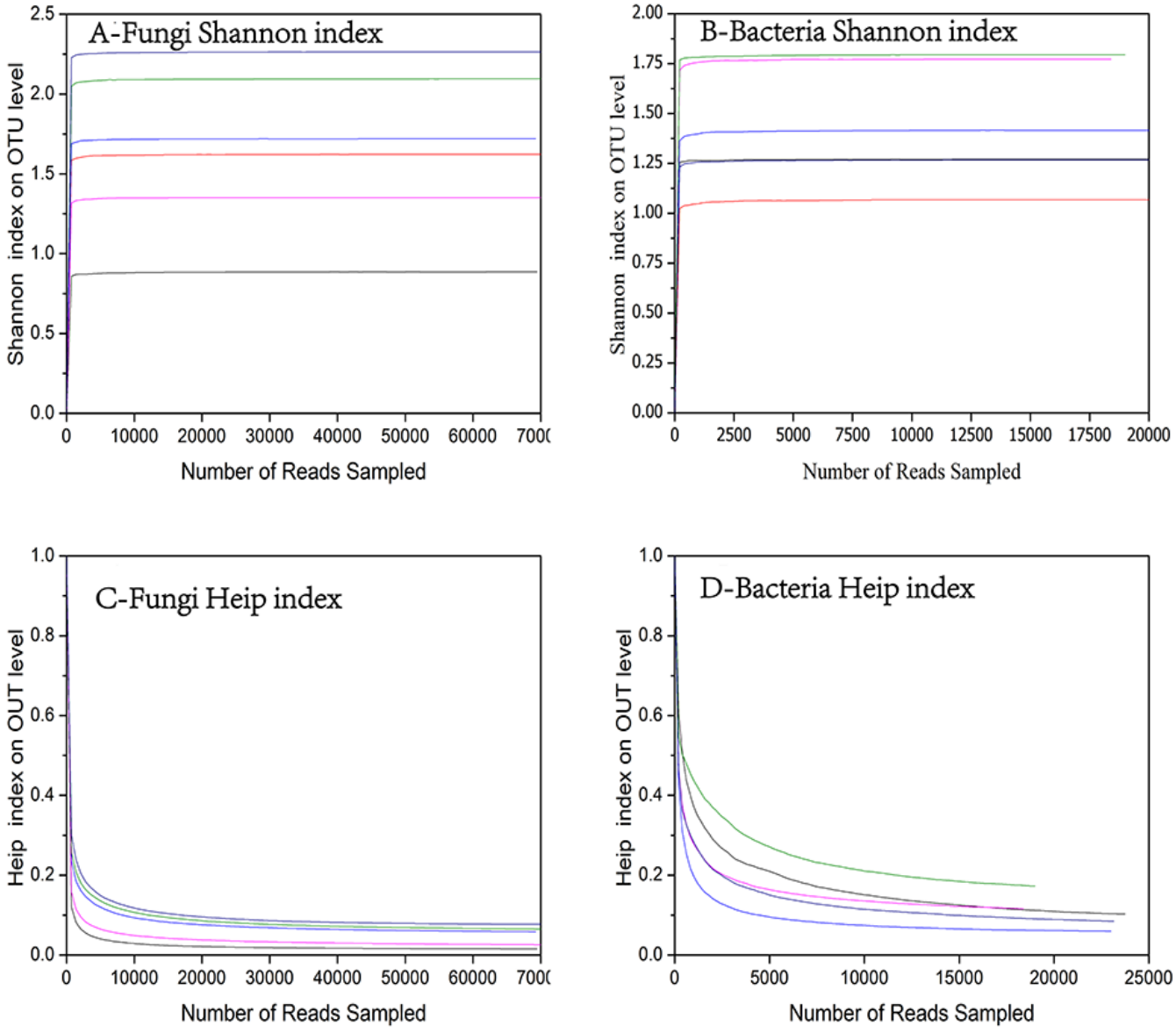

Figure 2

Shannon and Heip index curve of samples

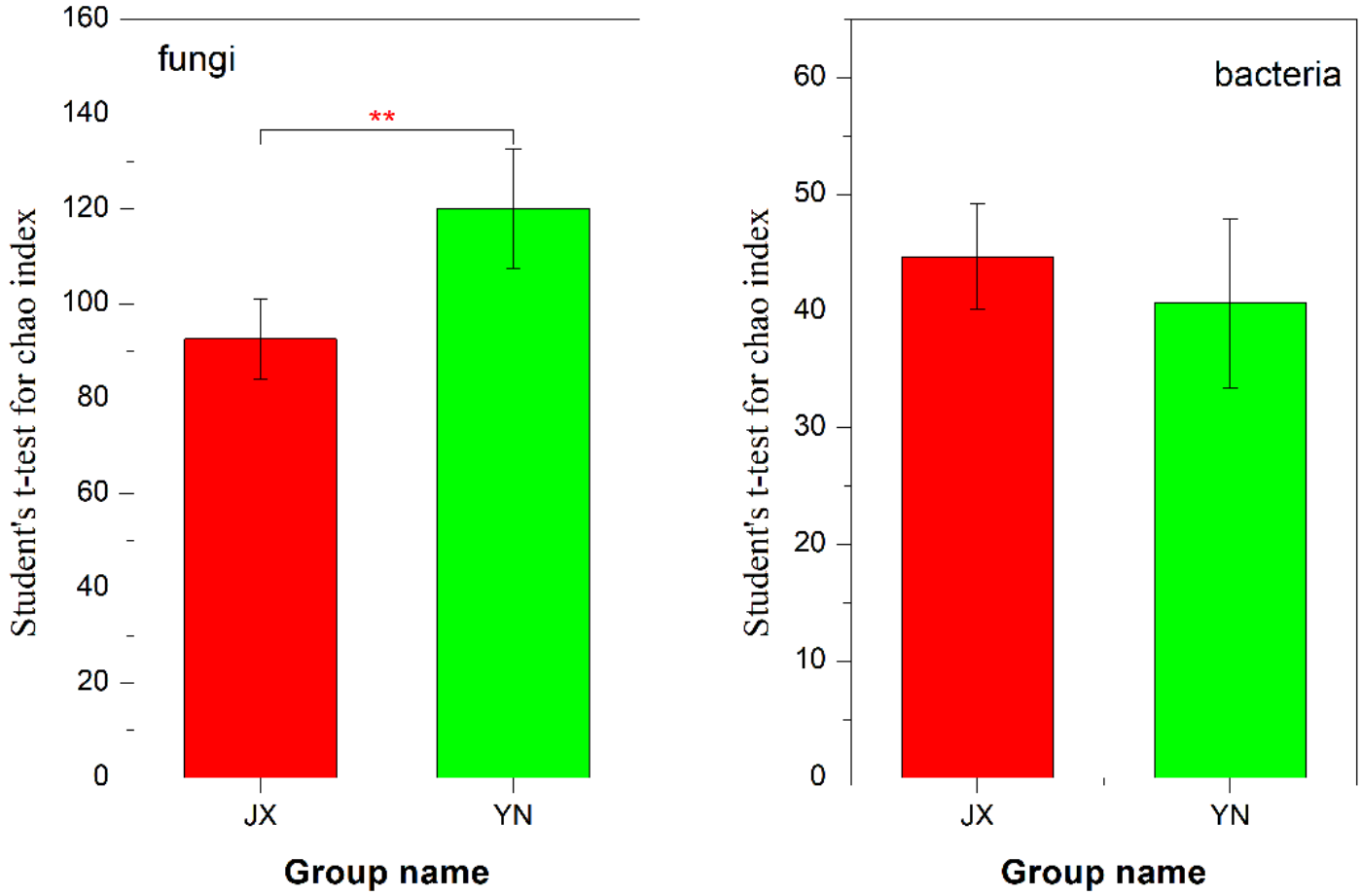

Figure 3

Inter group differences of different Cajanus cajan

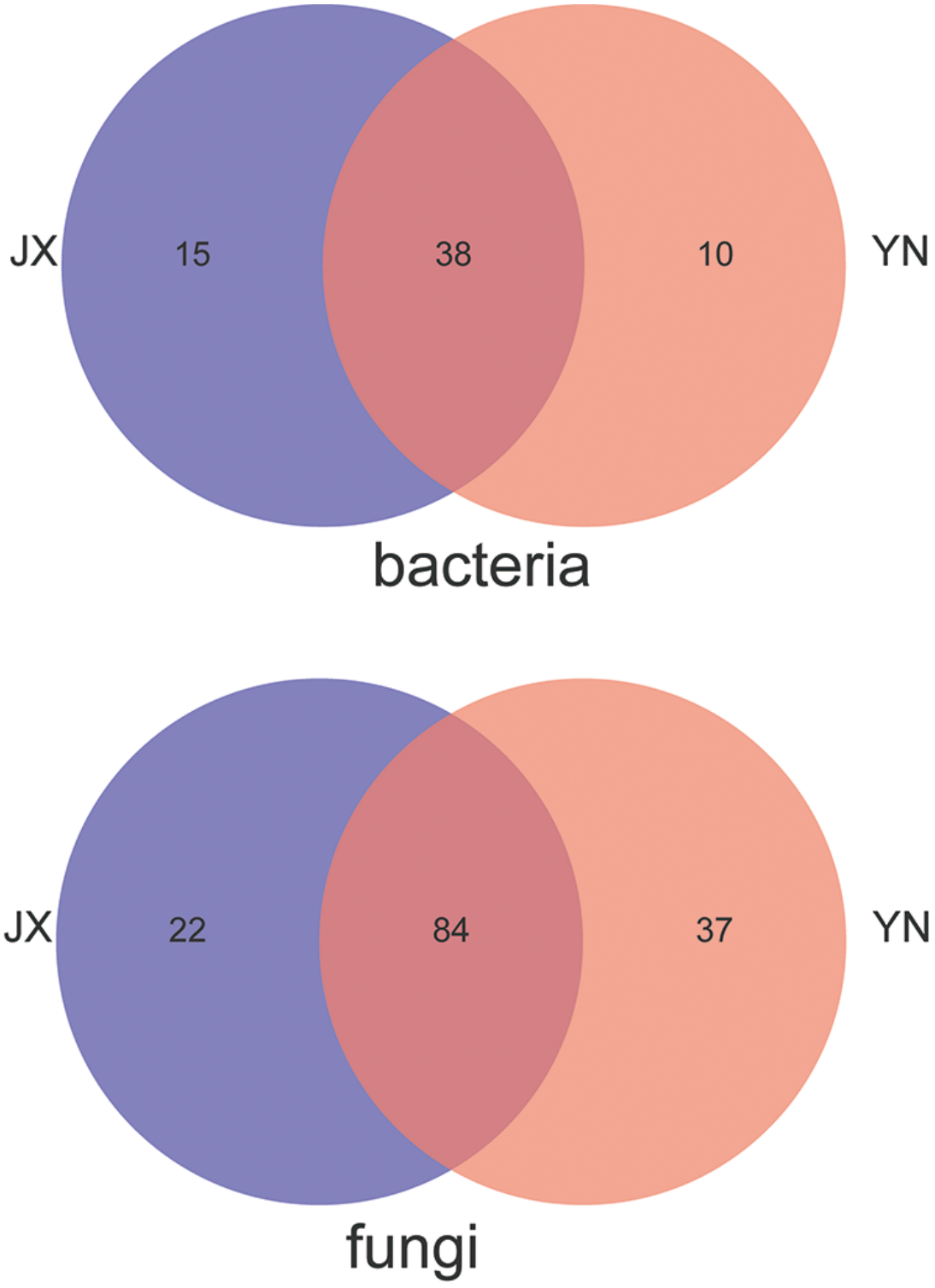

Figure 4

Venn charts of different Cajanus cajan on genus level

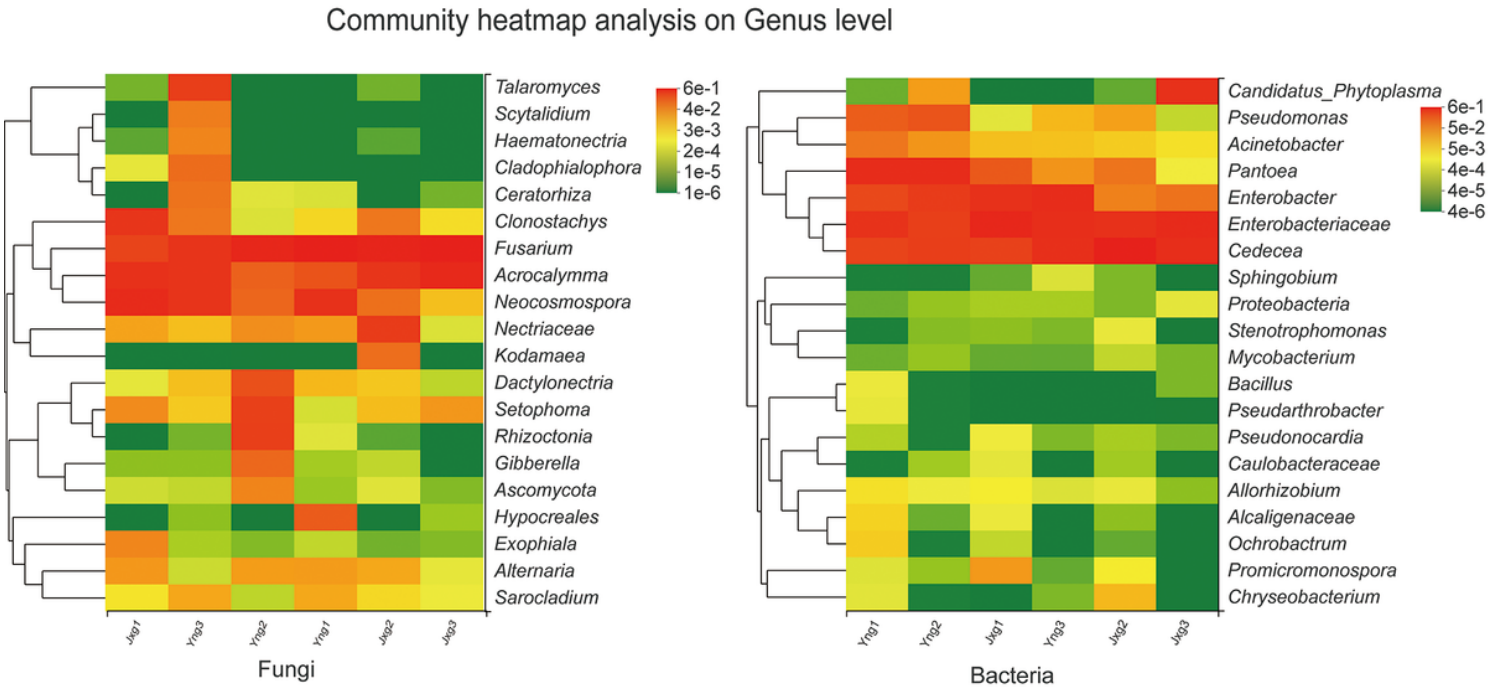

Figure 5

Community heat map analysis on genus level for different samples

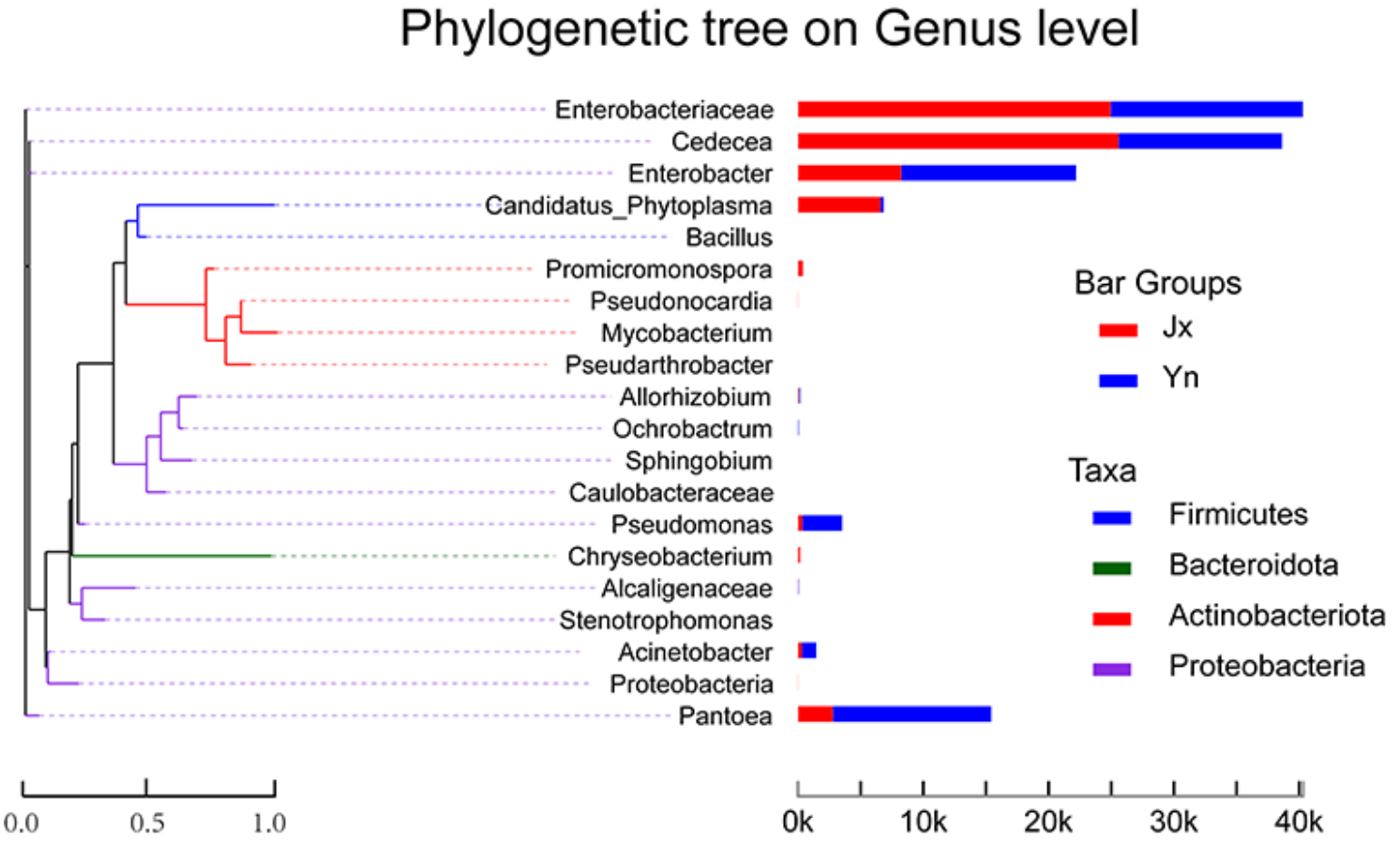

Figure 6

Phylogenetic trees of rhizobacteria on genus level

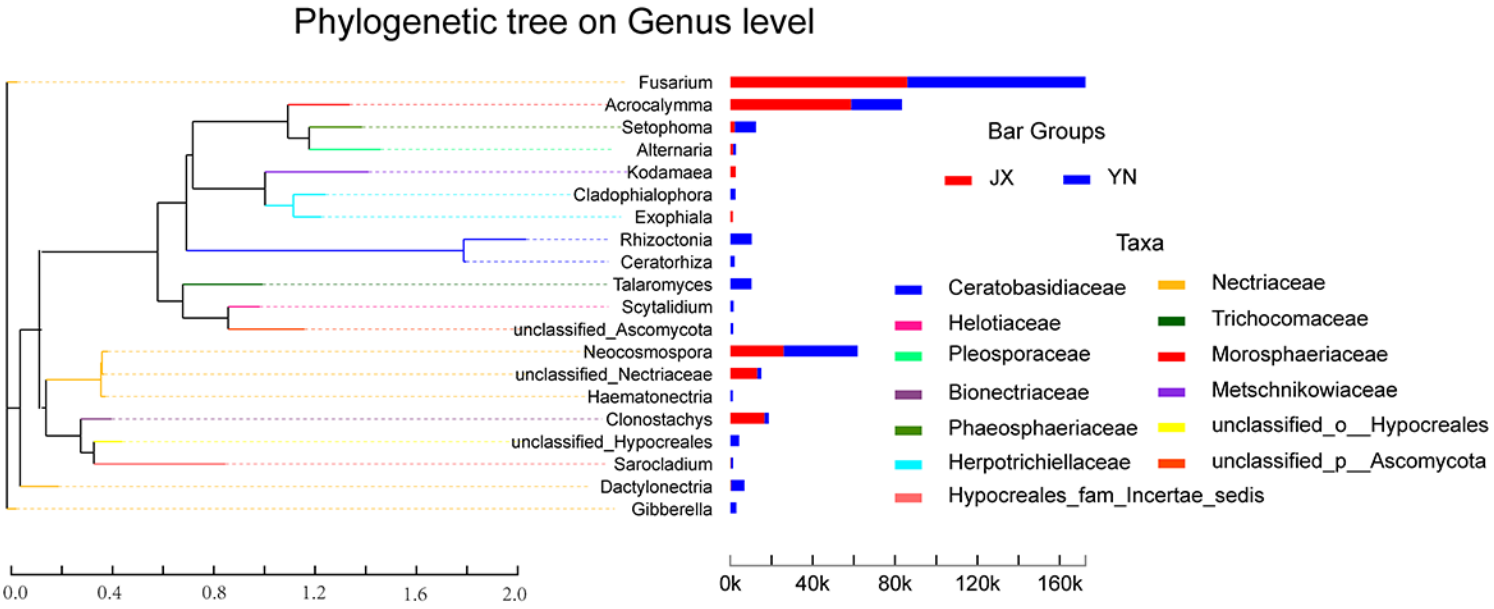

Figure 7

Phylogenetic trees of fungi on genus level

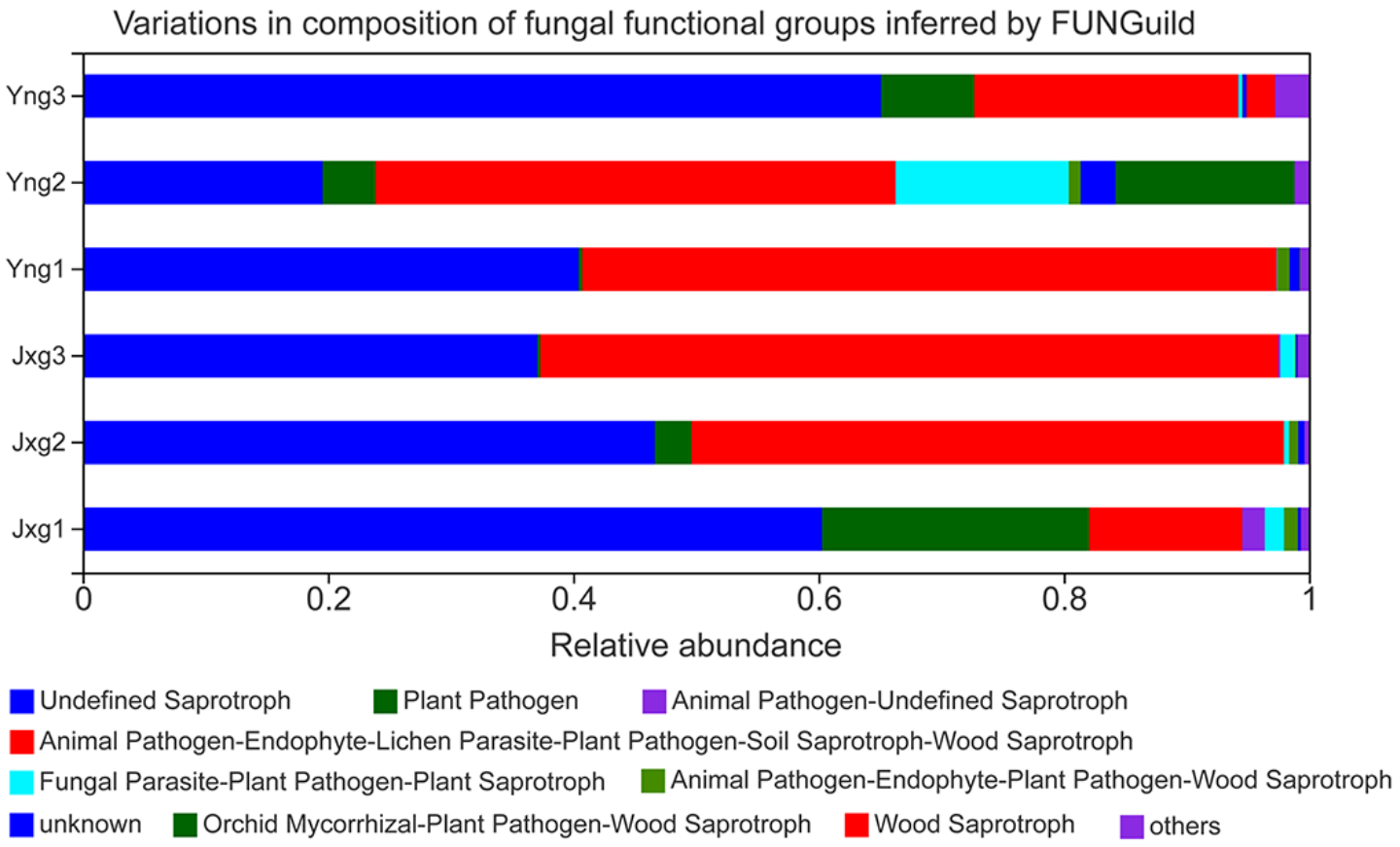

Figure 8

Variation in composition of fungal functional groups

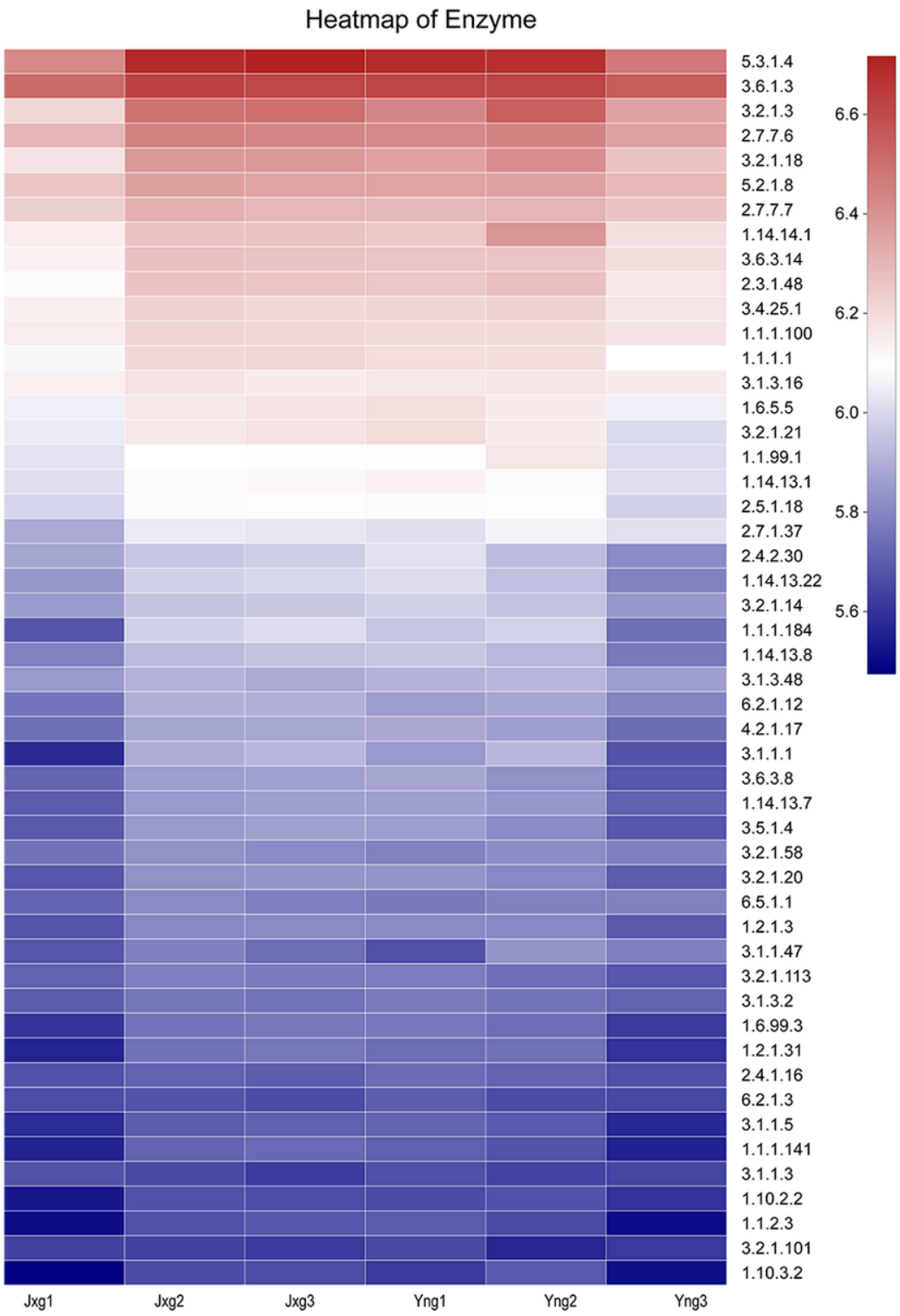

Figure 9

Heatmap of Enzyme in Fungi

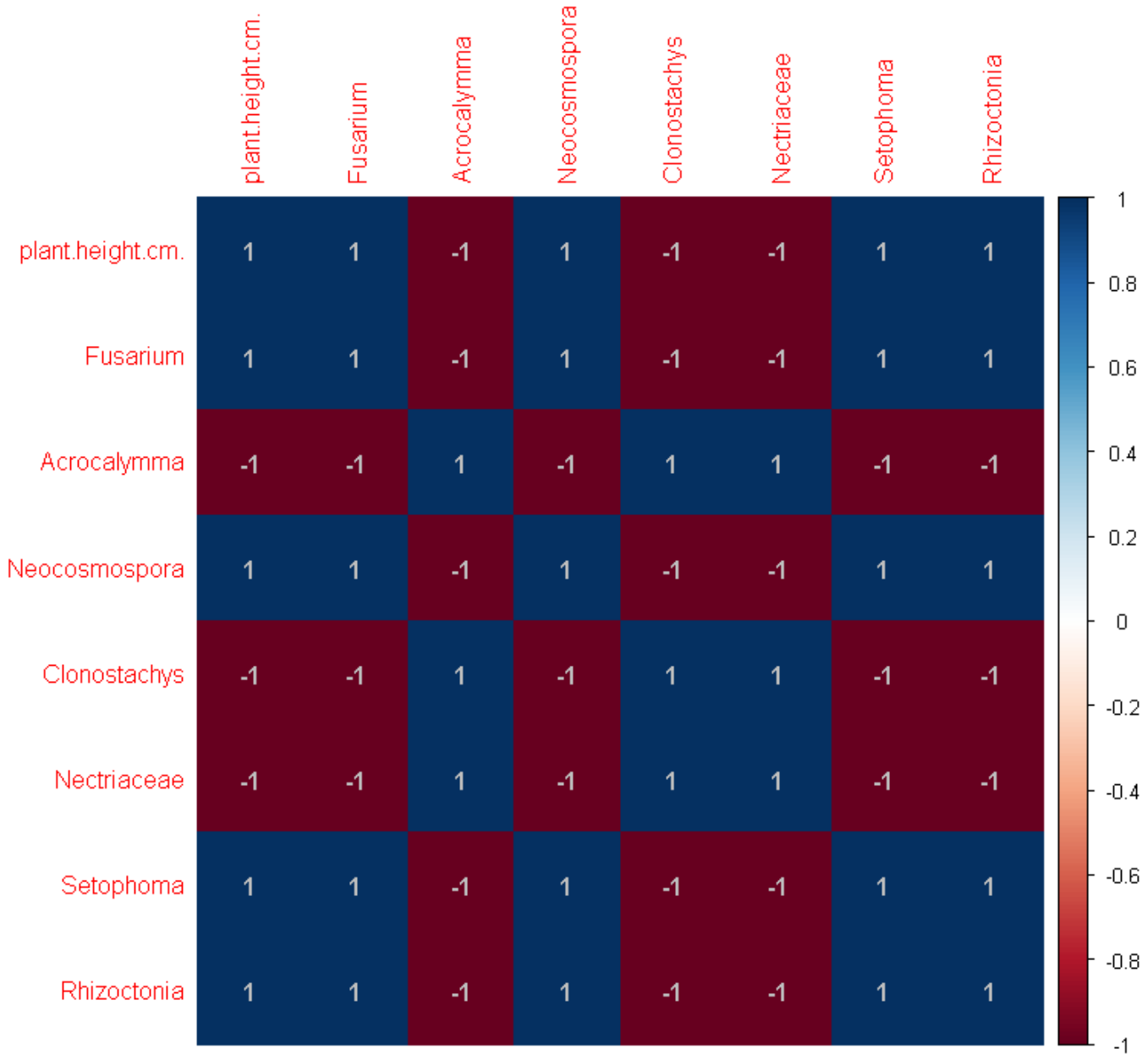

Figure 10

Heatmap of plant height and microorganism